8-2011

Analysis of Chlamydia Pneumoniae and AD-like Pathology in the Brains of BALB/c Mice Following Direct Intracranial Infection with Chlamydia Pneumoniae

Jessica Rachel Barton
Philadelphia College of Osteopathic Medicine, Jessicaba@pcom.edu

Philadelphia College of Osteopathic Medicine

M.S. in Biomedical Sciences

Department of Pathology, Microbiology, Immunology and Forensic Medicine

ANALYSIS OF *CHLAMYDIA PNEUMONIAE* **AND AD-LIKE PATHOLOGY IN THE BRAINS OF BALB/C MICE FOLLOWING DIRECT INTRACRANIAL INFECTION WITH** *CHLAMYDIA PNEUMONIAE*

A Thesis in Biomedical Sciences by Jessica Rachel Barton

Submitted in Partial Fulfillment of the Requirements for the Degree of

Masters in Biomedical Sciences

August 2011

We approve the thesis of Jessica Rachel Barton

_____ - _____.

C. Scott Little, Ph.D.
Associate Professor
Department of Pathology, Microbiology, Immunology and Forensic Medicine
Thesis Advisor

_____ - _____.

Marina D'Angelo, Ph.D.
Associate Professor
Department of Anatomy

_____ - _____.

Brian J. Balin, Ph.D.
Professor
Department of Pathology, Microbiology, Immunology and Forensic Medicine

_____ - _____.

Denah Appelt, Ph.D.
Professor
Department of Neuroscience, Physiology, Pharmacology

_____ - _____.

Marcus Bell, Ph.D.
Associate Professor
Department of Neuroscience, Physiology, Pharmacology
Program Director, Research Concentration
Master of Science in Biomedical Sciences

Abstract

Analysis of *Chlamydia pneumoniae* and AD-like Pathology in the Brains of BALB/c Mice Following Direct Intracranial Infection with *Chlamydia pneumoniae*

Jessica Rachel Barton

MS in Biomedical Sciences, August 2011

Department of Pathology, Microbiology, Immunology and Forensic Medicine

Philadelphia College of Osteopathic Medicine, Philadelphia, PA

C. Scott Little, Ph.D. Thesis Advisor

Alzheimer's disease (AD) is an age-related progressive neurodegenerative disorder and the most common form of dementia. The pathology in the central nervous system (CNS) impairs memory and cognition, hindering the capabilities and the quality of life of the individual. This project continues studying the role of infection and Alzheimer's disease and contributes to the overall understanding of the possible causes of this disease. In this study, BALB/c mice were infected, via direct intracranial injection, with a respiratory isolate (AR-39) of *Chlamydia pneumoniae*. Their brains were analyzed at 7 and 14 days post-infection, using immunohistochemistry, for the presence of *C. pneumoniae*, amyloid deposits and activated glial cells. The goal of this project was to measure the location and degree of *C. pneumoniae* burden, amyloid deposition and glial cell activation in the CNS following direct intracranial injection and to compare this data with results obtained from previous studies in this laboratory. We hypothesized that *C. pneumoniae* antigen and activated inflammatory cells will be observed in the infected

mouse brains following direct intracranial injection and Aβ deposition will be observed in areas where inflammation occurs. *C. pneumoniae*, amyloid deposits and activated glial cells were detected in the brains following direct intracranial infection with *C. pneumoniae*. At 7 days post-infection the average number of *C. pneumoniae*-specific immunoreactive sites was 68 ± 51.06 for the infected mice and, at 14 days post-infection, the average was 60 ± 43.79 for the infected mice. Within 0.84 mm of Bregma, the location of the injection, 166 of 203 total *C. pneumoniae*-specific immunoreactive sites (82%) and 26 of 27 (96%) total amyloid deposits were detected at 7 days post-infection. At 14 days post-infection, 126 of 179 total *C. pneumoniae*-specific immunoreactive sites (70%) and 13 of 32 (41%) total amyloid deposits were detected (within 0.84 mm of Bregma). From 7 to 14 days post-infection the *C. pneumoniae* and amyloid deposits located near the injection site spread distally from this location to other regions of the brain. These data confirm that *C. pneumoniae* is capable of establishing an infection in the CNS. Although deposits were observed, the lack of a substantial amount of amyloid deposits suggested that the generation of deposits may require longer than 14 days following *C. pneumoniae* infection. As early as 7 days post-infection, inflammation is observed in response to the presence of *C. pneumoniae* and/or soluble amyloid in the CNS and the contribution of both infection with *C. pneumoniae* and the presence of soluble amyloid elicit the inflammatory response that presumably precedes and contributes to amyloid deposition.

TABLE OF CONTENTS

LIST OF FIGURES

LIST OF TABLES

ACKNOWLEDGEMENTS

I would first like to express my gratitude to my thesis advisor, Scott Little, Ph.D. for his guidance, support and patience throughout this year. I would also like to thank my committee members, Denah Appelt, Ph.D., Brian Balin, Ph.D. and Marina D' Angelo, Ph.D. for their advice and hard work, which greatly contributed to my ability to successfully complete this project. I am appreciative of all of the assistance, advice and technical support Chris Hammond, M.S. offered continuously throughout this year. In addition, I would like to thank the Department of Pathology, Microbiology, and Immunology for providing an opportunity to better understand the study of Alzheimer's disease and research at Philadelphia College of Osteopathic Medicine (PCOM). Being a part of this laboratory and institution has been an incredible experience and will contribute to my ability to succeed as a medical student at Philadelphia College of Osteopathic Medicine as a part of the Class of 2015.

Introduction

I. Alzheimer's Disease

Alzheimer's disease (AD), the most common form of dementia in elderly individuals, is an age-related, progressive neurodegenerative disease that produces memory loss and severe cognitive impairment [1-3]. This form of dementia accounts for 50-60% of all dementia cases, currently affecting more than 15 million people worldwide [2]. According to the 2010 annual report from the Alzheimer's Association, 5.3 million people in the United States (U.S.) are suffering from this disease and the U.S. is currently spending approximately 172 billion dollars per year on associated costs [4]. This number of affected individuals and the associated costs places a clear strain on the healthcare system and society as a whole. Alzheimer's disease greatly impacts the quality of life of the individual, their family members, friends and caregivers. Throughout the past century significant progress in the study of AD has been made, which contributes to our understanding of AD and our ability to slow the progression of the disease in patients. However, it is important to build upon past research and gather new information so that the cause, and ultimately the cure, for AD can be determined.

II. Forms of Alzheimer's Disease and Neuropathology

In 1911, Alois Alzheimer described Alzheimer's disease as a mental disorder in elderly individuals characterized by two lesions in the brain. His work led to further investigations of individuals with this disorder and research that has contributed to our observation and understanding of the two forms of AD: familial, early-onset (FAD) and sporadic, late-onset AD (LOAD). Familial AD, which typically occurs prior to age 65, is an autosomal dominant disorder [2]. In contrast the onset of LOAD is not primarily due to a genetic disorder and instead it increases with age, generally occurring after age 65. Late-onset AD is much more prevalent than FAD, accounting for approximately 95% of all AD cases [3, 5].

Neuropathology shared by the two forms of AD presents as two defining hallmarks of the disease: neurofibrillary tangles (NFTs) and neuritic (senile) plaques (NSPs). Tangles are paired filaments of the abnormally hyperphosphorylated form of the tau protein, which accumulate in the perikaryal cytoplasm of neuronal cells. Plaques are extracellular accumulations of amyloid β (Aβ) peptide [3, 6-8]. The presence of Aβ plaques is thought to lead to neuronal dysfunction and death. The deposition of these plaques may promote hyperphosphorylation of tau and elicits a local inflammatory response, both of which will also contribute to additional injury and death of neurons [3].

Although we do not know what the function of amyloid β peptide is after normal processing, we do know that the peptide is produced throughout life and is derived from

the amyloid precursor protein (APP). The amyloid precursor protein is a transmembrane protein that has cleavage sites for the following enzymes: α-secretase, β-secretase and γ-secretase [3]. If APP is cleaved by α-secretase and γ-secretase Aβ formation is prevented, but if APP is cleaved by β-secretase and γ-secretase then the result is Aβ generation (Figure 1).

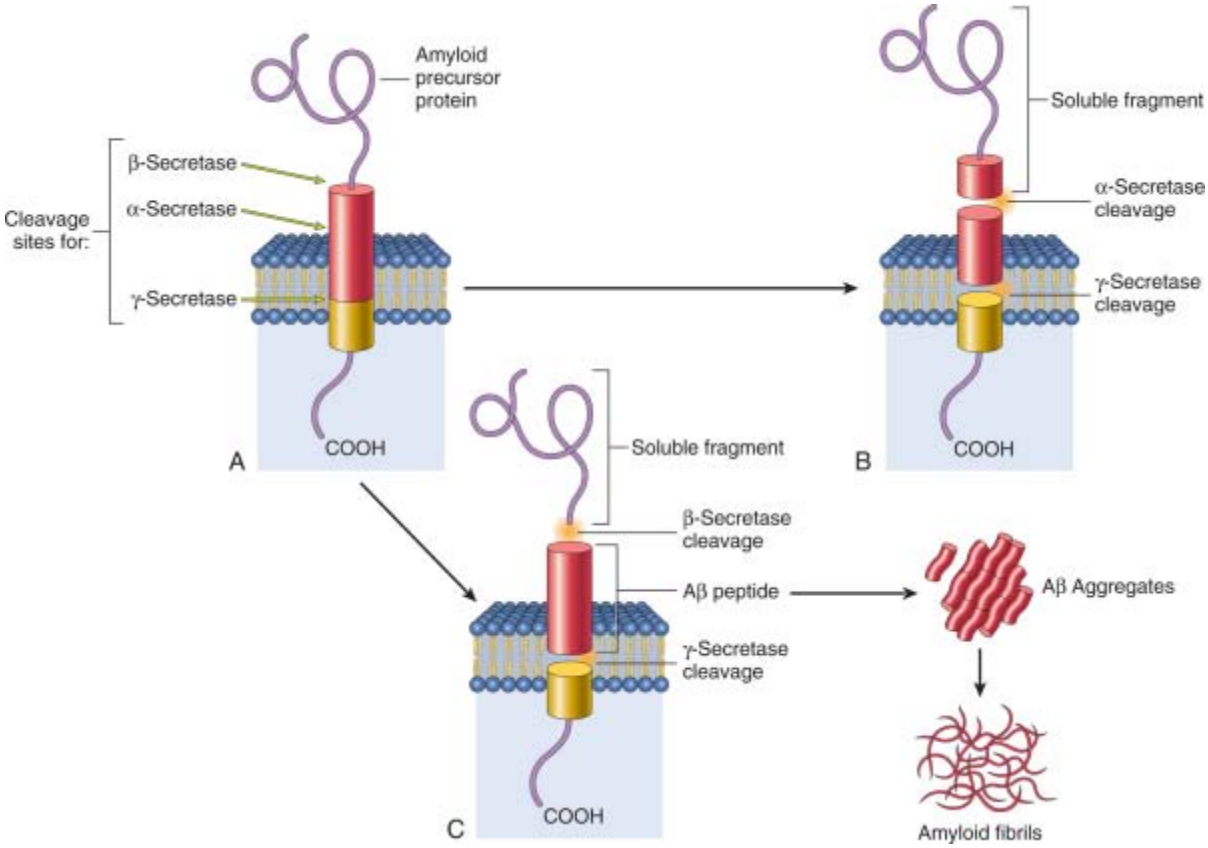

[3]

Figure 1. Amyloid Precursor Protein (APP) Proteolytic Cleavage

A) APP is synthesized in many cells and expressed as a transmembrane protein at the cell surface. When APP is present at the surface of the cell there are three enzymes - α-, β- and γ- secretase – that function to cleave this protein at corresponding cleavage sites on APP. B) Cleavage by α-secretase releases a soluble portion of APP into the extracellular environment and γ-secretase cleaves APP so that a portion remains internalized in the cell. C) When β- and γ-secretases act on APP, Aβ will be produced and released into the extracellular environment where it will readily form fibrils of Aβ peptide [3].

Generation of Aβ produces monomers of $A\beta_{1\text{-}40}$ and $A\beta_{1\text{-}42}$ [9]. Amyloid $\beta_{1\text{-}40}$ is the major form of cellular Aβ in the brain and is fairly soluble compared to $A\beta_{1\text{-}42}$, the

longer form of this peptide, which is fairly insoluble [10]. Amyloid β peptides, $A\beta_{1-40}$ and $A\beta_{1-42}$, are found in both normal and AD brains; however the proportions and the extent of burden differ. Plaques are composed of silver-staining neuritic processes that surround an extracellular deposit of Aβ, also known as the central amyloid core of the plaque [3]. Amyloid β_{1-42} aggregates more readily to form the central amyloid core in NSPs than $A\beta_{1-40}$ and is considered to be toxic to neurons [9, 10]. As all individuals age, Aβ will accumulate in the brain as the rate of Aβ formation increases with age. This rate increase is presumably due to a change in enzymatic activity, which is supported by previous observations in FAD cases [3].

Genetic risks have been linked to both forms of the disease. Individuals suffering from FAD have genetic defects that affect these pathways and cause Aβ to accumulate earlier and more rapidly. Familial AD involves mutations in APP and the transmembrane proteins presenilin-1 (PS-1) and presenilin-2 (PS-2) genes, all of which will lead to altered processing and thus accumulation of Aβ peptides in the brain [2, 5, 7]. These mutations are not responsible for LOAD, however, an association between apolipoprotein E (ApoE) ε4 allele and onset of LOAD has been recognized [2, 5, 11, 12]. The presence of this allele does not guarantee development of the disease as seen with the direct correlations between genetic mutations and onset of familial Alzheimer's disease. Two additional ApoE alleles, ε2 and ε3, generate the ApoE2 and ApoE3 isoforms, but it is the ε4 allele that accounts for the highest genetic risk associated with the development and rate of progression of LOAD [2].

Individuals who have the ε4 allele are at greater risk for developing LOAD and their cognitive functioning declines more rapidly than those lacking this allele, however,

people who do not have this allele may still get AD [13]. Due to the ability of this isoform to bind to Aβ, ApoE4 may contribute to plaque formation and reduction of Aβ clearance [14]. Those who have the genotypes ε2/ε4, ε3/ε4 and ε4/ε4 are at increased risk for the development of AD [15]. The ε3 allele is the most common of the three alleles, accounting for approximately 75% of all alleles and ε2 is the least common accounting for only about 10% [12, 14]. Individuals with genotypes ε2/ε2 or ε2/ε3 have a decreased risk of developing the disease and the age of onset of AD is typically later compared to individuals that possess one or more ε4 alleles [14, 15]. As previously mentioned, the presence of the ε4 allele does not guarantee AD development. The presence of this allele increases one's risk of developing AD which is diagnosed based on cognitive function and memory impairment and confirmed at autopsy.

III. Diagnosis and Clinical Manifestations

Alzheimer's disease is diagnosed using cognitive evaluations in living patients and is only confirmed at autopsy. A number of tests for evaluation and diagnosis, such as the mini mental status exam (MMSE), test various areas of cognitive function at the time the first symptoms are recognized, as well as over time to track the course of cognitive decline in the patient [16, 17].

Advancements in in-vivo technology, including magnetic resonance imaging (MRI) and positron emission tomography (PET), aid in the detection of changes of pathology in the central nervous system (CNS) and allow for comparison of healthy brains with those of individuals diagnosed with the disease. These imaging systems identify atrophy of the hippocampus and entorhinal cortex in human AD brains of living patients, which is supported by post-mortem examination upon death [2]. Although diagnosis of AD is only confirmed at autopsy, neuronal degeneration and the production of the two hallmark pathologies begins much earlier in specific regions of the brain leading to observable changes in the mental and physical status of the patient; and thus the clinical diagnosis of the disease in a living person [2, 16, 17].

The clinical manifestations of AD, such as loss of memory and cognitive decline, result from the dysfunction and death of neuronal cells, which will disrupt the biological processes in the affected regions of the brain, eventually spreading to the entire brain by the end-stage of the disease [16, 18]. Pathologic changes begin in the transentorhinal

cortex and the olfactory bulb is also thought to be one of the first areas affected [13], subsequently extending into the amygdala and hippocampal formation. Pathology can be observed in the frontal, temporal and occipital association areas as well. Ultimately pathology extends into the cerebral cortex, including the isocortex and neocortex [18, 19].

In 1991, Braak and Braak defined AD as a series of four stages that illustrates the progression of pathology and changes in various brain regions, a system widely utilized amongst AD researchers today. According to their research, the transentorhinal cortex, located between the entorhinal cortex and temporal isocortex, contains the first nerve cells affected in most cases of Alzheimer's disease. Following these observations they found pathology in and further involvement of the entorhinal region and the hippocampus. At this point they found that the isocortex still remains mostly unaffected. Pathology may also be observed in frontal, temporal and occipital association areas at this stage of the disease. Extensive pathology in the transentorhinal, entorhinal and hippocampal regions is expressed and their final stage describes pathology extending into the isocortex in addition to the previously mentioned affected regions [18].

Clinicians find that the clinical symptoms in the patient are consistent with the regions of the brain affected by neuronal degeneration and pathology over the course of this progressive neurodegenerative disease. For example, current studies have found pathology in the olfactory bulbs very early in the disease, which is consistent with some of the first symptoms of AD including lost sense of taste and smell [13]. AD patients initially present with extreme impairment of recent memory and decreased cognition,

which is consistent with pathology in the limbic system, which includes the entorhinal region, hippocampus and amygdala [5, 19, 20]. The hippocampus is an area of the brain critical in the formation of new memory, the entorhinal cortex is the primary source of afferents to the hippocampus, and the amygdala is involved in the emotion-related aspects of memory and learning [19]. Many researchers have contributed to our understanding of the pathology observed in and the clinical diagnosis of AD, however, the underlying causes of this disease are not as well-defined.

IV. Possible Causes of Alzheimer's Disease

The progress that has been made allowing us to understand, diagnose and treat Alzheimer's disease is remarkable. However, we are still working to discover the cause of LOAD so that we may eventually be able to determine a cure for the disease. A number of hypotheses have been proposed to explain the onset of Alzheimer's disease. The hypothesis that has the most data to support it is the amyloid cascade hypothesis [21].

a. Amyloid Cascade Hypothesis

The proposal of the amyloid cascade hypothesis plays a major role in AD research today as the focus shifts for some laboratories from treating AD to determining the cause of this disease. It was proposed by J. Hardy and G. Higgins, and also supported by D. Selko, in the early 1990's and states that there is an imbalance between production and clearance of Aβ ultimately leading to Aβ deposition, promoting neuronal degeneration and dysfunction, which is characteristic of both familial and sporadic forms of AD [2, 21, 22]. This hypothesis has been widely accepted since the finding that mutations in the genes for APP and presenilins, which are the substrate and enzyme for Aβ generation, have been implicated in FAD [2, 13]. As previously stated, the genetic mutations identified in patients with FAD are not responsible for the development of LOAD, but the neuropathology observed in both forms of the disease is identical.

There are many cases of elderly individuals who have extensive Aβ deposition identified at autopsy, even though they never presented with the clinical symptoms of AD while living [22, 23]. The amyloid cascade hypothesis correlates well with FAD where we observe onset of this form of AD as pathology increases. However, this hypothesis does not always fit for late-onset Alzheimer's disease since the amount of pathology is not always associated with the time of onset of the disease. Therefore, although Aβ may be involved in the pathophysiology of LOAD, it is only part of a larger picture. The initiating events leading to the onset of LOAD are not as well understood as those

contributing to FAD onset. Further research is necessary to determine the causative factors for the development of the late-onset form of the disease.

b. Infection

Neuropathology in both FAD and LOAD are similar, however, the reason this pathology is observed in the brains of individuals with LOAD remains unclear. Multiple possible causes of LOAD, a multifactorial disease, are recognized, including the role of infectious organisms. Researchers working to determine the cause of LOAD have observed an association between pathology in the AD brain and the onset of neuroinflammatory processes, which locally up-regulate inflammatory mediators when damaged neuronal cells, plaques and tangles are present [5-7, 24]. These studies support the fact that the brain, similar to other tissues in the body, is susceptible to infection. Furthermore, infectious agents can take several routes of entry to the CNS and may cause damage by directly injuring cells in the nervous system or through an indirect pathway/process that produces adverse effects due to an inflammatory or immune-mediated response [3, 13, 23].

In the study of LOAD, several viral and bacterial pathogens have been studied for their ability to establish an infection in the CNS that may contribute to neuropathology seen in Alzheimer's disease [13, 25]. Infection with *Herpes simplex virus type 1* (HSV-1) has been identified as a risk factor for the development of AD in certain individuals [25]. These are the individuals with at least one of the ε4 alleles for the ApoE gene. This

is the allele that accounts for the highest genetic risk for the development and rate of progression of late-onset Alzheimer's disease [2].

c. *Chlamydia pneumoniae*

Our laboratory focuses on infection with *C. pneumoniae,* a bacterial pathogen gaining significant attention for its role in numerous chronic diseases, in particular AD [7, 23, 26, 27]. *Chlamydia pneumoniae* is an obligate intracellular bacterial pathogen that infects mucosal surfaces of the respiratory tract [28-30]. *C. pneumoniae* is generally transmitted person-to-person through aerosolized droplets to the respiratory tract and can disseminate systemically, typically infecting and "hitching a ride" inside monocytic cells, although it has been shown to be capable of infecting an array of human cell types [13, 23, 31, 32]. Like other chlamydial species, *C. pneumoniae* is characterized by a biphasic developmental cycle. The first phase is defined by the activity of an infectious metabolically inactive elementary body (EB) attaching to target cells of the host and uptake into a vacuole, and the second phase by a dividing, intracellular, metabolically active reticulate body (RB). The developmental cycle starts with the conversion of EB to the growth form, RB, which then divides and usually reverts back to the EB form and is released from the host cell to continue propagating the infection [5, 13, 29].

Chlamydia pneumoniae infection has been associated with the onset and progression of several chronic diseases [13, 33]. For example, studies have observed a correlation between infection with this organism and coronary artery disease as

C. pneumoniae has been identified in plaques associated with atherosclerosis [26, 34]. Adult populations that have been tested show seroprevalence over 40% worldwide [32, 33]. This organism is wide-spread in society often producing infections that are asymptomatic and in response to the host immune reaction the organism adapts and enters a persistent/non-replicative state, which may promote a chronic infection. It is thought that the pathogenesis of this persistent state may be associated with chronic disease development [13, 29].

This lab has developed a mouse model of AD-like pathology in which amyloid deposits have been experimentally induced following infection with a human AD-isolate of the organism *C. pneumoniae* [5, 7]. This model is useful for exploring the early events that take place in LOAD as well as the role of infection, particularly with the organism *C. pneumoniae*, in the induction of neuroinflammation and AD pathogenesis.

In recent experiments [7], BALB/c mice were infected, intranasally, with a respiratory isolate of *C. pneumoniae* (AR-39) and their brains were isolated following perfusion at 1, 2, 3, or 4 months post-infection (unpublished observations). Brains of experimentally infected or mock-infected age and sex matched mice were analyzed via immunohistochemistry using antibodies specific for amyloid or *C. pneumoniae* antigens. The greatest amount of *C. pneumoniae* was detected at 1 month post infection, and then decreased at 2, 3 and 4 months post infection. The amount of Aβ deposition peaked at 2 months post-infection, which suggests that *C. pneumoniae* is capable of establishing a CNS infection and promoting amyloid deposition, which may serve as a stimulus for inflammation in the brain. Therefore, the presence of amyloid plaques in the brains of

the infected mice was likely a consequence of an inflammatory response to infection (unpublished observations).

d. Inflammation

Chronic inflammation is a hallmark of AD, however, whether the inflammatory response results from the over expression of Aβ or other stimuli is yet to be determined [26]. The accumulation of Aβ in the CNS leads to amyloid β deposits, a key feature of the pathogenesis of Alzheimer's disease. Amyloid β is known to lead to the dysfunction and death of neuronal cells in its presence [3, 9]. The initiating factors of LOAD are still unknown, but research in this laboratory suggests that infection may be the initial source for inflammation and thus the development of AD-like pathology [7, 13].

The resident immune and phagocytic cells of the CNS, microglia, are the initial sensors of pathogens or changes in the brain environment [35]. Microglia are stimulated by the presence of soluble amyloid, the type present prior to forming a deposit, or insoluble amyloid, deposits or plaques [9, 17]. Microglia and astrocytes are capable of binding both soluble and insoluble amyloid, via specific receptors that are recognized by the Aβ peptide, and Aβ aggregates have also been shown to activate microglia and astrocytes [24, 35]. Following binding to Aβ, microglia become "activated," which is defined as cells that have an altered shape and size of their cell bodies, lengths of their processes, as well as functional changes compared to "resting" microglia. Once in the

active state, the microglia will phagocytize any material they recognize as disrupting the homeostasis of the CNS, including amyloid. Microglia will also respond by secreting inflammatory mediators and proteolytic enzymes or neurotrophic factors that influence astrocytes, another type of glial cell, and neurons inducing secondary inflammatory responses [9, 35]. The glial response will resolve once infection is cleared or damaged tissues have been repaired, thus preventing disease in the short term. However, when the presence of the inflammatory stimulus persists or the normal resolution mechanisms fail, sustained or chronic inflammation results and this glial response may contribute to the progression of disease [35].

The role of glia in AD is still not well understood, but astrogliosis and changes in microglia morphology that are observed in AD brains provides evidence of an inflammatory response in AD [35]. Studies using transgenic mouse models for AD have shown that the amount of microglia in the CNS increases with increased levels of amyloid plaques, as early as two months of age [36]. Another group [37], working with a β-site APP cleavage enzyme (BACE1) [3] transgenic mouse model of AD, has observed microglial activation earlier than two months of age and even before observing the presence of amyloid deposits in the CNS . This illustrates the possibility that microglia may respond to altered APP processing that can lead to eventual accumulation of amyloid in the CNS [37]. The ability of microglia to detect and respond to injury or the presence of pathogens in the brain is crucial for maintaining homeostasis and consequently normal processing and functioning in the CNS. However, continuous activation of these immune cells may lead to chronic inflammation and thus the progression of disease [9, 38].

Both the high prevalence of infection with *C. pneumoniae* in the population and the presence of inflammation in the CNS, a common observation in both *Chlamydia*-induced diseases and the AD brain, led this laboratory to its decision to investigate a possible relationship between *C. pneumoniae* and Alzheimer's disease in the late 1990's. Several studies in this laboratory have also confirmed the presence of *C. pneumoniae* in areas of the AD brain presenting with neuropathology [7, 13, 26]. Balin et al compared postmortem brain samples from patients with and without AD and found that in brain areas with typical AD related neuropathology 89% of the AD patients were positive for *C. pneumoniae* and 95% of the non-AD control brains were negative for this organism [26]. Another group studying the response of microglia to infection with *C. pneumoniae*, [38], observed an increase in the number of activated microglial cells in the brains of *C. pneumoniae* PCR-positive mice compared to infected PCR-negative and mock infected mice. Based on the data obtained and the correlations observed between *C. pneumoniae* and AD in previous experiments, this lab continues investigating the role of infection with this organism and late-onset Alzheimer's disease. This laboratory is working to confirm that inflammation induced following infection with *C. pneumoniae* promotes the generation and deposition of amyloid β.

V. Study Directive and Hypothesis

Previous experiments have illustrated the ability of *C. pneumoniae* to get into the CNS and produce AD-like pathology (Aβ 1-42) [7, 11, 26]. Although Aβ 1-42 deposits were detected via immunohistochemistry, it did not co-localize with *C. pneumoniae* in these studies, suggesting the inflammatory response to the presence of *C. pneumoniae* may play a role in Aβ 1-42 formation.

This laboratory has not previously studied the effects of direct intracranial infection with *C. pneumoniae* in model animals for Alzheimer's disease. This project aims to expand on the knowledge and data gained from our previous studies, where mice were infected intranasally. We will investigate the presence of *C. pneumoniae* antigen, activated glial cells and Aβ deposition in fixed and embedded mouse brain tissue that was previously infected, via direct intracranial injection, with *C. pneumoniae*. The goal of the proposed research is to measure the location and degree of amyloid deposition, *C. pneumoniae* antigen and glial cell activation in the CNS following direct intracranial injection.

To contribute to our understanding of the role of infection with *C. pneumoniae* in AD this project aims to:

1) determine the amount of pathogen needed to initiate/produce pathology

2) determine the mobility of the pathogen in the CNS once present

3) determine the presence and location of activated glial cells and compare this to regions where *C. pneumoniae* and/or Aβ is observed

4) compare these results with previous data in order to further elucidate how this may contribute to progressive pathology in other regions of the brain

We hypothesize that C. pneumoniae antigen and activated inflammatory cells will be observed in the infected mouse brains following direct intracranial injection and Aβ deposition will be observed in areas where inflammation occurs.

Materials and Methods

I. *Chlamydia pneumoniae*

BALB/c mice were infected with 1 x 10^5 infectious units, of a human respiratory isolate of *C. pneumoniae*, AR-39, obtained from the American type Culture Collection (ATCC), and propagated in HEp-2 cells, isolated for these experiments. Infectious units were administered via direct intracranial injection. Hank's balanced salt solution (HBSS) vehicle alone was given intracranially for age and sex matched uninfected control mice. (Table 1)

II. Infection of Mice and Brain Removal

Female BALB/c mice were infected, intracranially, with *C. pneumoniae*. The injection site is located at approximately Bregma -2.12mm on the anatomical right side of the mouse brain (Figure 2). At 7 or 14 days post-infection the mice were sacrificed and perfused with 4% paraformaldehyde. Their brains were immersion fixed in 4% paraformaldehyde for more than 48 hours. The fixed tissue was embedded in paraffin and then sectioned coronally at 7-10 microns thickness.

III. Mouse Brain

A total of 50 brain coronal sections were immunolabeled per mouse: 4 sets (1 per primary antibody) and 1 set (secondary antibody only) for both the rostral and caudal portions of the brains – 5 sections were labeled for each set. The immunolabeled sections were 7-10 microns thick and spaced equally at 35-50 micron intervals. Samples represent regions spanning from rostral (bregma + 2.22mm) to caudal (bregma – 5.88mm). (Figure 3)

IV. Antibodies

Primary antibodies specific for *C. pneumoniae*: mouse monoclonal RDI-PROAC1p used at a working concentration of 1:10 (Research Diagnostics Incorporated, Flanders, NJ), mouse monoclonal M6600 also used at a working concentration of 1:10 (DakoCytomation, Carpinteria CA), and mouse monoclonal 10C-27 used at a working concentration of 1:100 (Fitzgerald, Concord MA). Primary antibodies specific for amyloid beta 1-42 antigens: rabbit polyclonal Aβ 1-42 used at a working concentration of 1:300 (Oncogene Research Products) and mouse monoclonal Aβ 1-42 (6E10) used at a working concentration of 1:500 (Covance). The primary antibody specific for glial fibrillary acidic protein (GFAP) was mouse, anti-human monoclonal GFAP used at a working concentration of 1:25 (AbD Serotec, Raleigh, NC). Alkaline phosphatase conjugated secondary antibodies were utilized to visualize the respective antigens of

interest. All antibodies were diluted to working concentration in phosphate buffer saline – blocking buffer (Table 2).

V. Immunohistochemistry

Coronal sections (see Materials and Methods subsection *Mouse Brain*) were re-hydrated by melting the wax for 30 seconds, followed by xylene – 3 minutes (3x) (Thermo Fisher Scientific, Pittsburgh PA), rehydrated in a series of graded alcohol solutions – 100% ethanol for 3 minutes (2x), 90% ethanol for 3 minutes (1x) and 70% ethanol for 3 minutes (1x) (Electron Microscopy Sciences, Fort Washington PA), followed by DI H_2O for 3 minutes. Next, slides were placed in Citra antigen retrieval buffer (BioGenex, San Roman CA) and steamed in a 2010 Retreaver (Pick Cell Laboratories, Amsterdam Netherlands) for 20 minutes at high pressure (120^{o}C). Slides remained in antigen retrieval buffer overnight at room temperature.

Slides were rinsed with phosphate buffer saline (PBS) pH 7.4 (Sigma-Aldrich, St. Louis MO) 3 x 5 minutes. Endogenous peroxidase activity was quenched utilizing a 3% solution of H_2O_2/PBS (stock 30%, Thermo Fisher Scientific, Pittsburgh PA) for five minutes at room temperature. Sections were rinsed 1 x 5 minutes in PBS and blocked three times in 2% heat inactivated fetal bovine serum (FBS)/PBS (Mediatech, Herndon VA). Primary antibodies Aβ1-42, Aβ6E10, mixed "cocktail" of 10C-27, AC1P, M6600, or GFAP (Table 2) were applied to tissue sections and placed in a humidified chamber at 37^{o}C for 90 minutes. The sections were rinsed 3 x 5 minutes each and then blocked 3 x 15 minutes each in 2% FBS/PBS, then incubated with appropriate secondary antibodies

in a humidified chamber for 60 minutes at 37^{o}C. Following incubation, sections were rinsed with distilled water 3 x 5 minutes and developed using alkaline phosphatase new magenta for fifteen minutes (BioFX, Owings Mills MD). Next, sections were rinsed in distilled water 3 x 5 minutes followed by one PBS rinse for 5 minutes. Acidified Harris's Hematoxylin (Mercury free) was applied to sections for 1 minute (Thermo Fisher Scientific, Pittsburgh PA). Sections were rinsed thoroughly in distilled water and then were contrasted in PBS for 5 minutes. The sections were rinsed with distilled water 3 x 5 minutes, air dried, and crystal mounted (BioMeda, Foster City CA) and air-dried overnight. Once dry, the sections were permounted (Fisher Chemicals, Fair Lawn NJ) and coverslipped.

VI. Microscopic Analysis

Microscopic examination of tissue was completed using 10x, 20x, 40x and 60x objectives. Digital still images were captured using NIS-Elements F 2.20 Imaging System software on a Nikon Eclipse 50i microscope using a Nikon Digital Sight DS-SM Camera.

VII. Mapping Immunolabeling on Mouse Coronal Schematics:

Each coronal section viewed was matched to a representative coronal section from the Mouse Brain Library (http://www.mbl.org/). These representative sections were used to illustrate immunolabeling seen in the corresponding brain section.

Table 1. Study design

	7 Days Post-Infection	14 Days Post-Infection
Control (no injection)	n=0/5	n=1/5
Control (vehicle)	n=1/1	n=0/1
Infected	n=3/5	n=3/5

A total of 11 mice were prepared for each time point – 5 control (no injection), 1 control (vehicle) and 5 infected. All of the infected mice were infected via direct intracranial injection with *C. pneumoniae*. The control mice were either injected with vehicle only (HBSS) or not injected. For this project a total of four mice were analyzed for the day 7 time point – one vehicle only control mouse and three experimental mice – and a total of four mice were analyzed for the day 14 time point – one no injection control and three experimental mice.

Table 2. Antibodies

Antibody Name	Supplier	Antigen Recognized	Conc. (mg/mL)	Species	Conjugate
AC1P RDI-PROAC1p (10R-C124a)	Research Diagnostics Incorporated, Flanders NJ (Fitzgerald, Concord MA)	Cpn lipopoly-saccharide	0.05	Mouse, monoclonal I_gG3	NA
M6600	DakoCytomation, Carpinteria CA	Cpn major outer membrane protein	1:10*	Mouse, monoclonal I_gG	NA
10C-27	Fitzgerald, Concord MA	Cpn	1.05	Mouse, monoclonal I_gG	NA
Aβ 1-42	Oncogene Research Products	Aβ 1-42	0.391	Rabbit, polyclonal I_gG	NA
Aβ 1-42 (6E10)	Covance	Aβ 1-42	1.0	Mouse, monoclonal I_gG	NA
GFAP	AbD Serotec, Raleigh, NC	Glial fibrillary acidic protein	1:25*	Mouse, anti-human, monoclonal I_gG1	NA
AP-Goat anti-mouse IgG	Zymed Laboratories, San Francisco CA	NA	2.0	Goat, anti-mouse	Alk, Phos.
AP-Goat anti-rabbit IgG	Zymed Laboratories, San Francisco CA	NA	2.0	Goat, anti-rabbit	Alk. Phos.

'Cpn' = *C. pneumoniae*. * No concentration was provided, only volumes were given by manufacturers, along with suggested working dilutions.

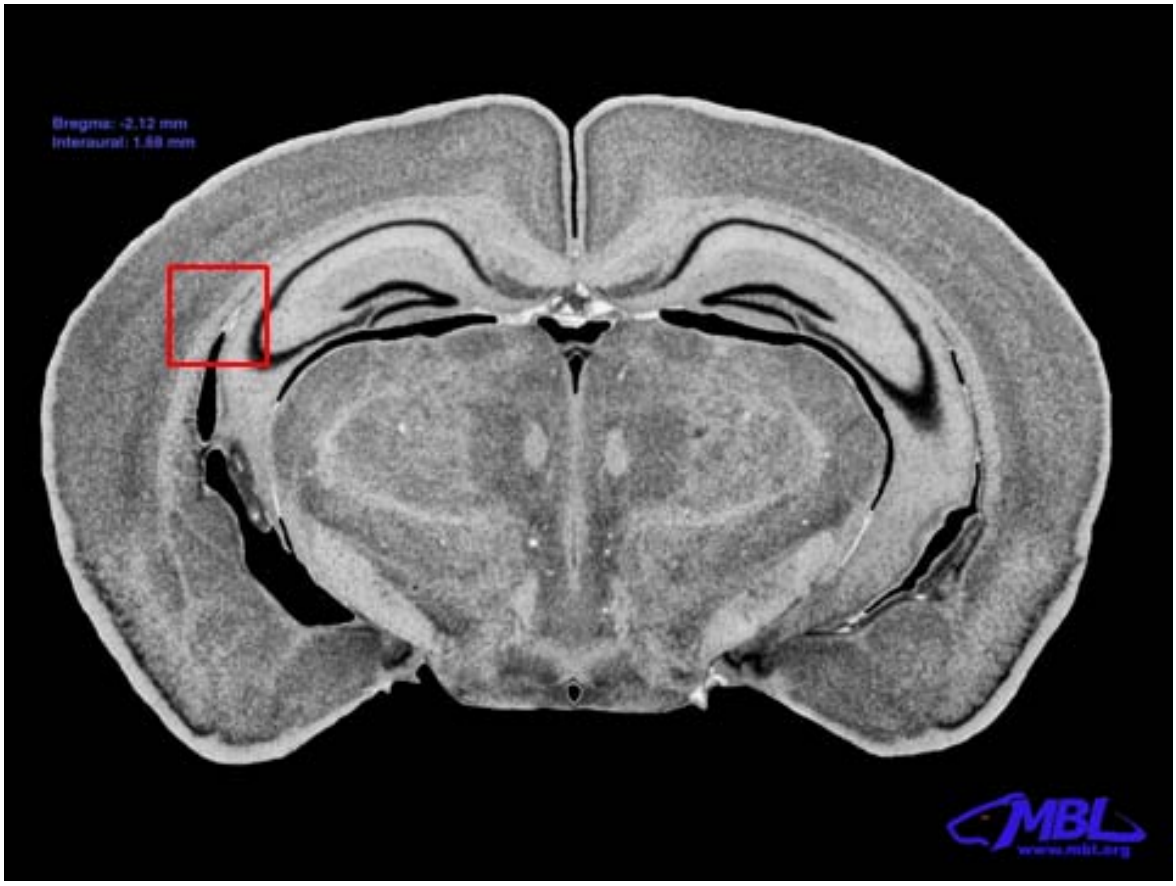

Figure 2. Injection Site.

The boxed area on the image above represents the approximate location of the injection site in the mouse brain – Bregma -2.12 mm [39].

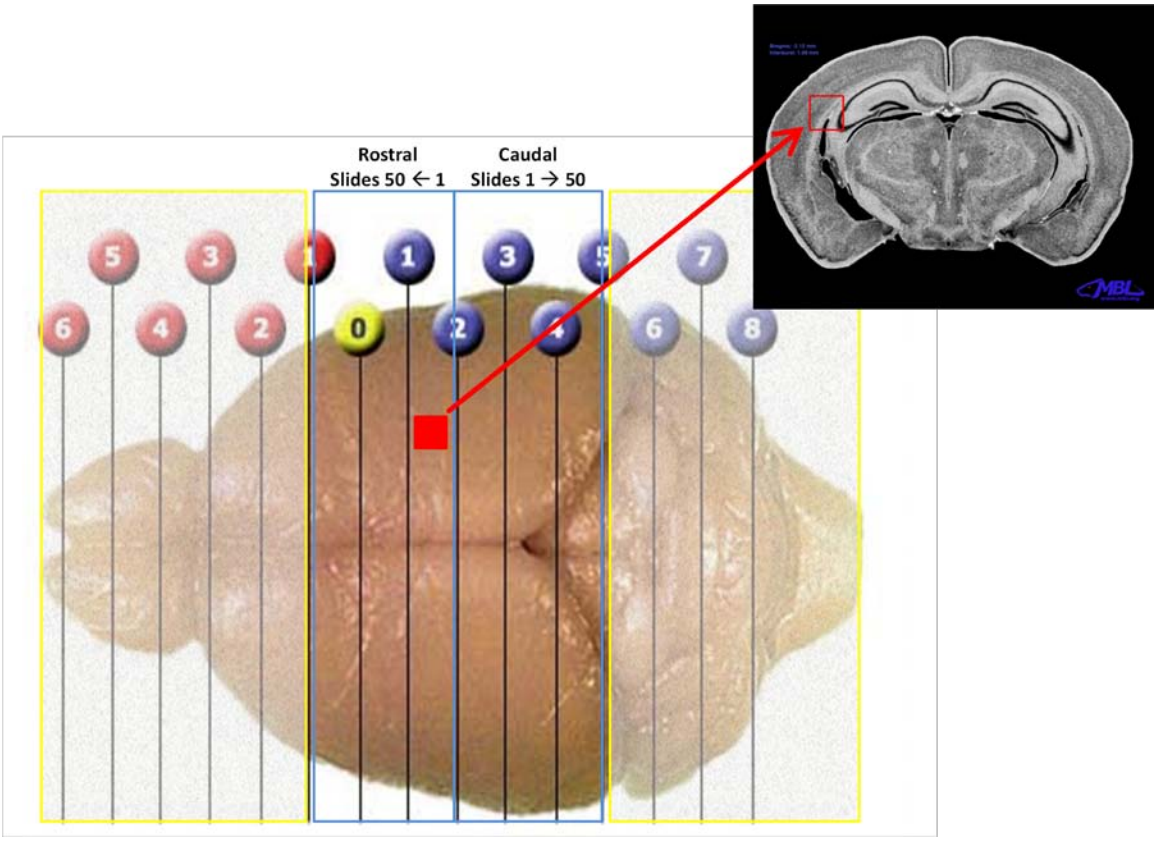

Figure 3. Anatomic Locations of Representative Coronal Sections

The numbers and corresponding lines above are 1 mm apart from one another. The regions boxed in red indicate the location of the injection site. The brains were sliced coronally starting, at line 2 above, approximately, and then separated into two halves – rostral (BrA) and caudal (BrB). From this initial slice (at line 2) the two halves were serially sectioned, every 35-50 microns and at a thickness of 7-10 microns, in both the rostral and caudal directions – see small arrows at the top of the figure [39].

Results

For each time point, 7 and 14 days post-infection, a total of 4 mice – 3 infected and 1 uninfected – were analyzed for the presence of *C. pneumoniae* antigen, amyloid deposits and activated glial cells.

I. Identification of *C. pneumoniae* Antigen in the CNS

Following direct intracranial infection, *C. pneumoniae* antigens were detected, via immunohistochemistry, in the CNS of the mice. As described earlier (see Materials and Methods subsection *Mouse Brain*), a total of 80 coronal brain sections, 10 per mouse, were immunolabeled for *C. pneumoniae* and analyzed via microscopy. Both typical intracellular *C. pneumoniae*-specific labeling (Figure 4B and 4C) and some atypical extracellular labeling (Figure 4A) was observed.

The day 7 time point included three mice infected with C. *pneumoniae* and one control mouse injected with vehicle only (HBSS). *C. pneumoniae* antigen was detected via immunohistochemistry in all mice at this time point (Table 3). Two of the three infected mice displayed 129 and 70 immunoreactive sites, which was greater than the 27 immunoreactive sites detected in the vehicle injected control, for this time point. A total of 4 immunoreactive sites were detected in the third infected mouse for this time point. The average *C. pneumoniae* antigen burden for the infected mice at this time point was 68 ± 51.06. Within 0.84 mm of Bregma (the location of the injection site) in both the rostral and caudal directions, 166 of 203 (82%) *C. pneumoniae*-specific immunoreactive

sites were detected (Table 5). *Chlamydia pneumoniae* was observed in regions of interest in AD, such as thalamus, hippocampus and entorhinal cortex, as well as areas not significantly affected early on in the disease (Figure 7, left column).

At 14 days post-infection histologic samples from three mice infected with *C. pneumoniae* and one no-injection control mouse were analyzed. Similar to what was observed at the day 7 time point, *C. pneumoniae* antigen was detected via immunohistochemistry in all mice at this time point (Table 3). Two of the three infected mice displayed 111 and 64 immunoreactive sites, greater than the 18 sites observed in the uninfected, no-injection, control mouse for this time point. The third infected mouse in this group had 4 immunoreactive sites. The average *C. pneumoniae* antigen burden for the infected mice at this time point was 60 ± 43.79. Only 126 of 179 (70%) *C. pneumoniae*-specific immunoreactive sites were detected proximal to the injection site, within 0.84 mm of Bregma (Table 5). *Chlamydia pneumoniae* was observed in regions of interest in AD, such as thalamus, hippocampus and entorhinal cortex, as well as areas not significantly affected early on in the disease (Figure 8, left column).

II. Identification of Amyloid Deposits in the CNS

Following direct intracranial infection with *C. pneumoniae*, a small number of amyloid deposits were observed, via immunohistochemistry, in the CNS of the mice. As described earlier (see Materials and Methods subsection *Mouse Brain*), a total of 160 coronal brain sections, 20 per mouse, were immunolabeled for amyloid β and analyzed via microscopy. Twice as many slides were analyzed for amyloid, compared to *C.*

pneumoniae. Two antibodies were used to label for amyloid in the CNS – 10 slides/antibody/per mouse (see Materials and Methods subsection *Antibodies*). The Aβ-specific immunolabeling observed (Figure 5) was comparable to Aβ-specific immunolabeling noted previously [7].

At 7 days post-infection histologic samples from three mice injected with C. *pneumoniae* and one control mouse injected with vehicle only (HBSS) were observed. Deposits were detected via immunohistochemistry in 3 of 3 infected mice, using the polyclonal Aβ-specific antibody and detected in 2 of 3 infected mice, using the monoclonal Aβ6E10 antibody. No deposits were observed in the uninfected mouse with either antibody, at this time point (Table 3). The average number of deposits for the infected mice at this time point using the Aβ 1-42 antibody was 4 ± 2.89 and with the Aβ6E10 antibody the average number of deposits was 5 ± 4.12. Within 0.84 mm of Bregma (the location of the injection site) in both the rostral and caudal directions, 26 of 27 (96%) total amyloid deposits were detected (Table 5).

The day 14 time point included three mice injected with *C. pneumoniae* and one mouse that served as the no-injection control. Deposits were detected via immunohistochemistry in 2 of 3 infected mice, using the polyclonal Aβ-specific antibody, and detected in 3 of 3 infected mice, using the monoclonal Aβ6E10 antibody (Table 3). Two deposits were observed in the uninfected mouse labeled with the Aβ 1-42 antibody. The average number of deposits for the infected mice at this time point using the Aβ 1-42 antibody was 5 ± 3.69 and with the Aβ6E10 antibody the average total number of deposits was 6 ± 4.32. Within 0.84 mm of Bregma (the location of the

injection site) in both the rostral and caudal directions, 13 of 32 (41%) total amyloid deposits were detected (Table 5).

III. Identification of Activated Glial Cells in the CNS

Activated glial cells were detected in the CNS of the mice, via immunohistochemistry, following direct intracranial infection with *C. pneumoniae*. As described earlier (see Materials and Methods subsection *Mouse Brain*), a total of 80 coronal brain sections, 10 per mouse, were immunolabeled with glial fibrillary acidic protein (GFAP)-specific antibody and analyzed via microscopy. For each mouse, the slides labeled with GFAP were matched to comparable representative coronal sections from the Mouse Brain Library (See Materials and Methods subsection *Mapping Immunolabeling on Mouse Coronal Schematics*). Activated glial cells were immunoreactive with GFAP-specific antibody and associated with a nucleus in the CNS (Figure 6, right column, see arrows). Regions of the brain section that contained a high density of activated glial cells were circled on the representative coronal sections (see green circles in Figure 6, left column and Figures 7 and 8, right columns).

At 7 and 14 days post-infection global activation of glia was observed in the CNS of infected mice. The number of regions with activated glial cells was greater in the infected mice compared to uninfected controls at both time points (Figure 6). The hippocampus and dentate gyrus, regions of the brain significant in AD, of infected vs. uninfected mice were compared. The comparison of tissue from an infected mouse to a control, or uninfected mouse, at each time point illustrates a substantial difference in total

number of activated glial cells (Figure 6, center column). Activated glial cells were observed in regions of interest in AD, such as thalamus, hippocampus and entorhinal cortex, as well as areas not significantly affected early on in the disease (Figures 7 and 8, right columns).

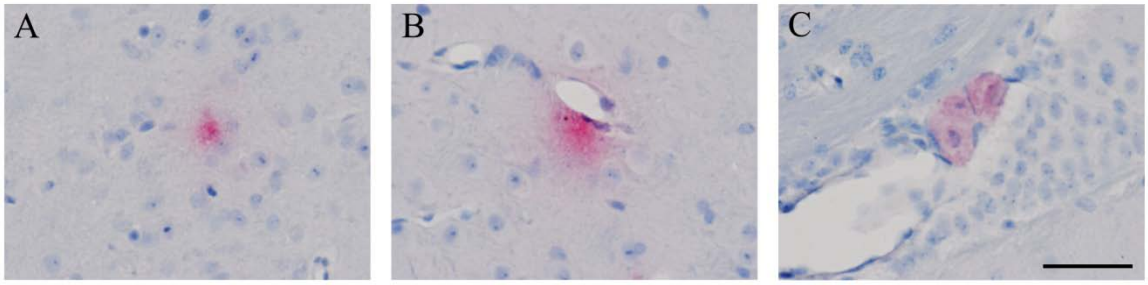

Figure 4. *C. pneumoniae*-specific labeling in the brains of intracranially infected mice

These images represent *C. pneumoniae* labeling, which includes extracellular and intracellular, observed in the brains of experimental mice at both 7 and 14 days post-infection. A) Representative image of extracellular labeling of *C. pneumoniae*. B) Representative image of labeling of *C. pneumoniae* associated with a blood vessel. C) Representative image of labeling of intracellular *C. pneumoniae*. (Size bar = 100 µm)

Table 3. Total amount of *C. pneumoniae*-specific labeling

	7 Days Post-Infection	14 Days Post-Infection
Control	27	18
Infected	129	111
Infected	4	4
Infected	70	64

The total amount of *C. pneumoniae*-specific immunoreactive sites observed at both 7 and 14 days post-infection is displayed above. The mean number of immunoreactive sites for the infected mice at day 7 was 68 ± 51.06 and the mean number of immunoreactive sites for the infected mice at day 14 was 60 ± 43.79.

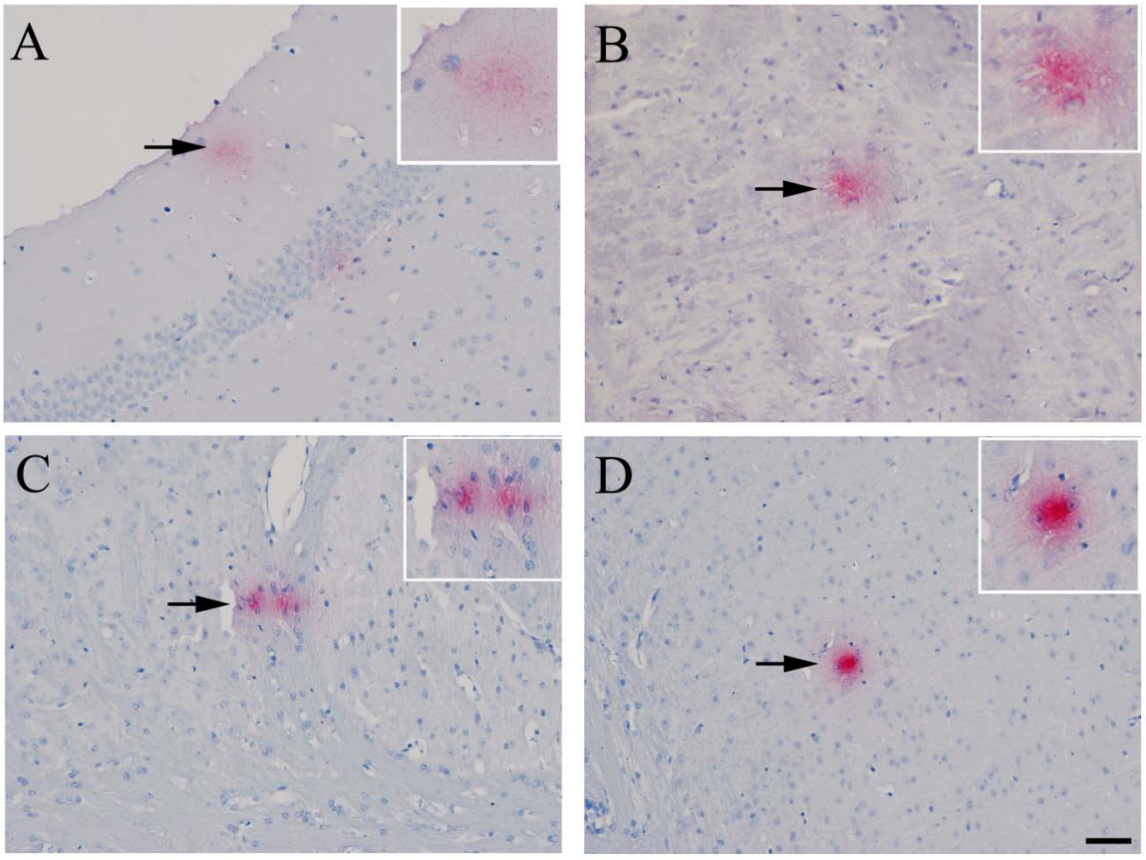

Figure 5. Amyloid deposits in the brains of intracranially infected mice

These images represent amyloid labeling observed for experimental mice at both 7 and 14 days post-infection. The top corners of each image are inset with a higher magnification image of amyloid deposits as designated by the low magnification arrow. A and B) Representative images of amyloid deposits observed using the Aβ 1-42 antibody are presented here. C and D) Representative images of amyloid deposits observed using the Aβ6E10 antibody are presented. (Size bar = 100 μm)

Table 4. Total number of amyloid deposits

	Total Amount of Aβ (7 Days Post-Infection)		Total Amount of Aβ (14 Days Post-Infection)	
	Aβ 1-42	**Aβ6E10**	**Aβ 1-42**	**Aβ6E10**
Control	0	0	2	0
Infected	8	4	5	4
Infected	1	0	9	2
Infected	4	10	0	12

The total number of amyloid deposits observed at both 7 and 14 days post-infection is presented here. Labeling with two antibodies specific for Aβ 1-42 antigen, Aβ 1-42 and Aβ6E10 (see Materials and Methods subsection *Antibodies*), were used to obtain this data. The mean number of deposits for the infected mice at day 7, using the polyclonal Aβ-specific antibody, was 4 ± 2.89 and for the infected mice, using the monoclonal Aβ6E10 antibody, the mean was 5 ± 4.12. At 14 days post-infection the mean number of deposits for infected mice, using the polyclonal Aβ-specific antibody, was 5 ± 3.69 and for the infected mice, using the monoclonal Aβ6E10 antibody, the mean was 6 ± 4.32.

Table 5. Distribution of *C. pneumoniae* and amyloid deposits

		Rostral ←								Bregma		→ Caudal					
	Section Locations (mm) →	**1.98**	**1.70**	**1.32**	**0.74**	**0.38**	**0.00**	**-0.82**	**-0.94**	**-1.28**	**-1.64**	**-2.12**	**-2.75**	**-2.92**	**-3.80**	**-4.20**	**-4.60**	**-4.92**
Day 7																		
Cpn Antigen	Control 27	-	-	-	-	-	-	-	-	**27**	**-**	**-**	**-**	**-**	-	0	0	0
	Experimental 203	-	-	-	-	-	-	-	1	**16**	**35**	**35**	**24**	**56**	33	-	2	1
Amyloid Deposits Aβ1-42 (Aβ6E10)	Control 0 (0)	-	-	-	-	-	-	-	-	**0 (0)**	**-**	**-**	**-**	**-**		0 (0)	0 (0)	0 (-)
	Experimental 13 (14)	-	-	-	-	-	-	-	0 (0)	**2 (8)**	**8 (1)**	**-**	**0 (5)**	**2 (0)**	0 (-)	1 (0)	0 (0)	-
Day 14																		
Cpn Antigen	Control 18	-	-	-	-	-	-	1	0	**6**	**-**	**2**	**9**	**-**	-	-	-	-
	Experimental 179	1	11	4	5	2	-	-	-	**11**	**9**	**-**	**-**	**106**	30	0	-	-
Amyloid Deposits Aβ1-42 (Aβ6E10)	Control 2 (0)	-	0 (0)	-	0 (0)	0 (0)	0 (0)	-	-	**0 (0)**	**0 (0)**	**-**	**-**	**2 (0)**	0 (0)	-		-
	Experimental 14 (18)	-(1)	0 (1)	1 (-)	0 (1)	5 (-)	3 (1)	-	-	**0 (3)**	**0 (7)**	**-**	**-**	**0 (3)**	5 (1)	- (0)	-	-

The distribution of *C. pneumoniae* (Cpn) immunoreactive sites and amyloid deposits in both infected and uninfected, control, mice at 7 and 14 days post-infection are displayed above. The total number of immunoreactive sites or deposits observed are listed beneath the designated group – control or experimental. For each time point there are control groups n=1 and the experimental groups n=3. Bregma, -2.12 mm, is the anatomical location of the injection site for the intracranial injections in the mice. The red text highlights the data selected as being proximal to the injection site (within 0.84mm of Bregma in both the rostral and caudal directions) and the other numbers in the table are considered as data that is distal to the injection site. The dashes (-) are placed in the table to indicate sections we did not have to analyze for this project. The data from both amyloid antibodies is expressed in the order: number of labels detected using Aβ1-42 (number of labels detected using Aβ6E10).

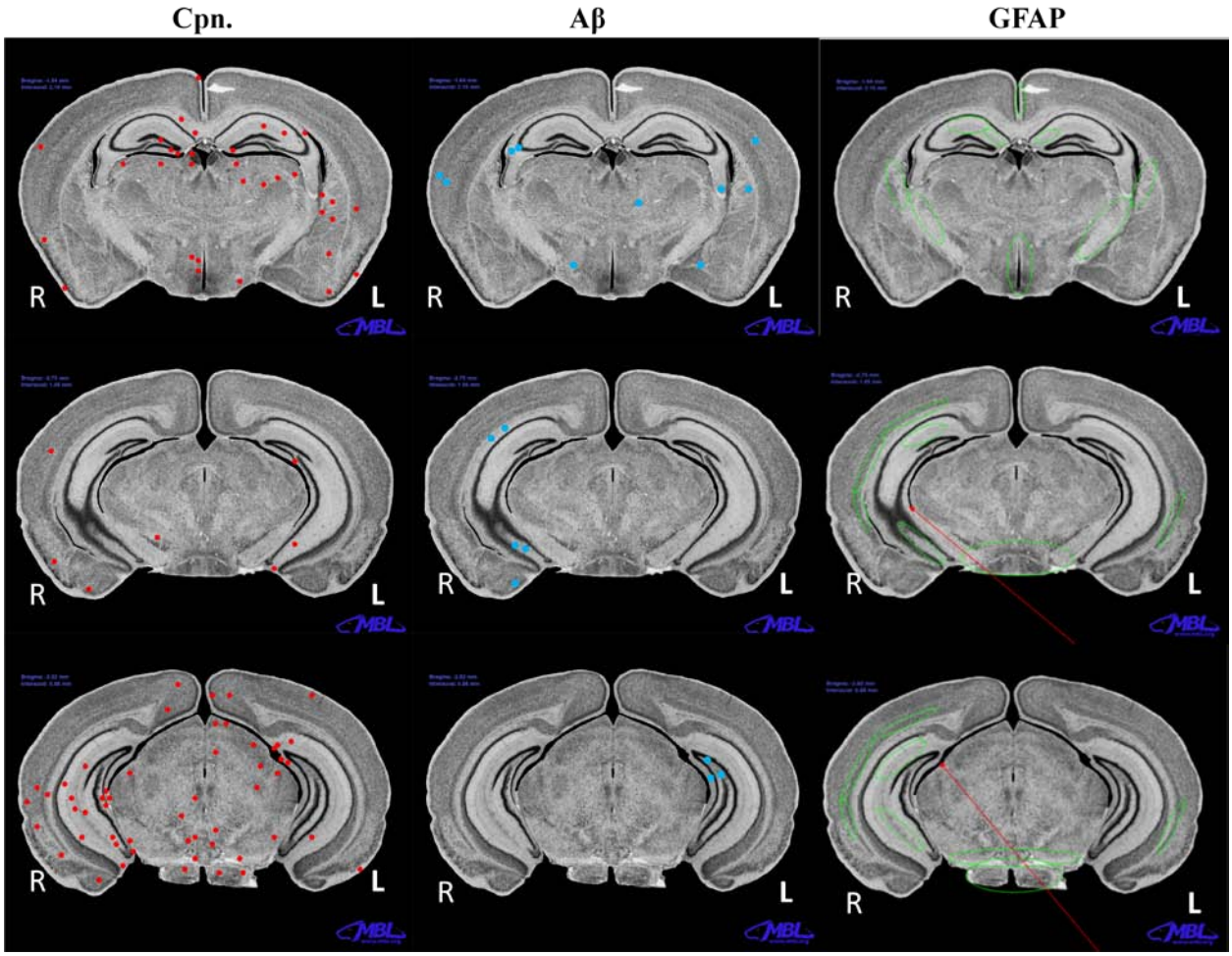

Figure 6. Distribution of *C. pneumoniae-specific* immunoreactive sites, amyloid deposits and activated glial cells at 7 days post-infection

C. pneumoniae immunoreactive sites (red dots), Aβ deposits (blue dots) and regions of the brain with glial cell labeling (green circles or red arrows) from individual slides in the day 7 group are presented here in areas of the hippocampus and dentate gyrus, as well as regions not affected early on in Alzheimer's disease.

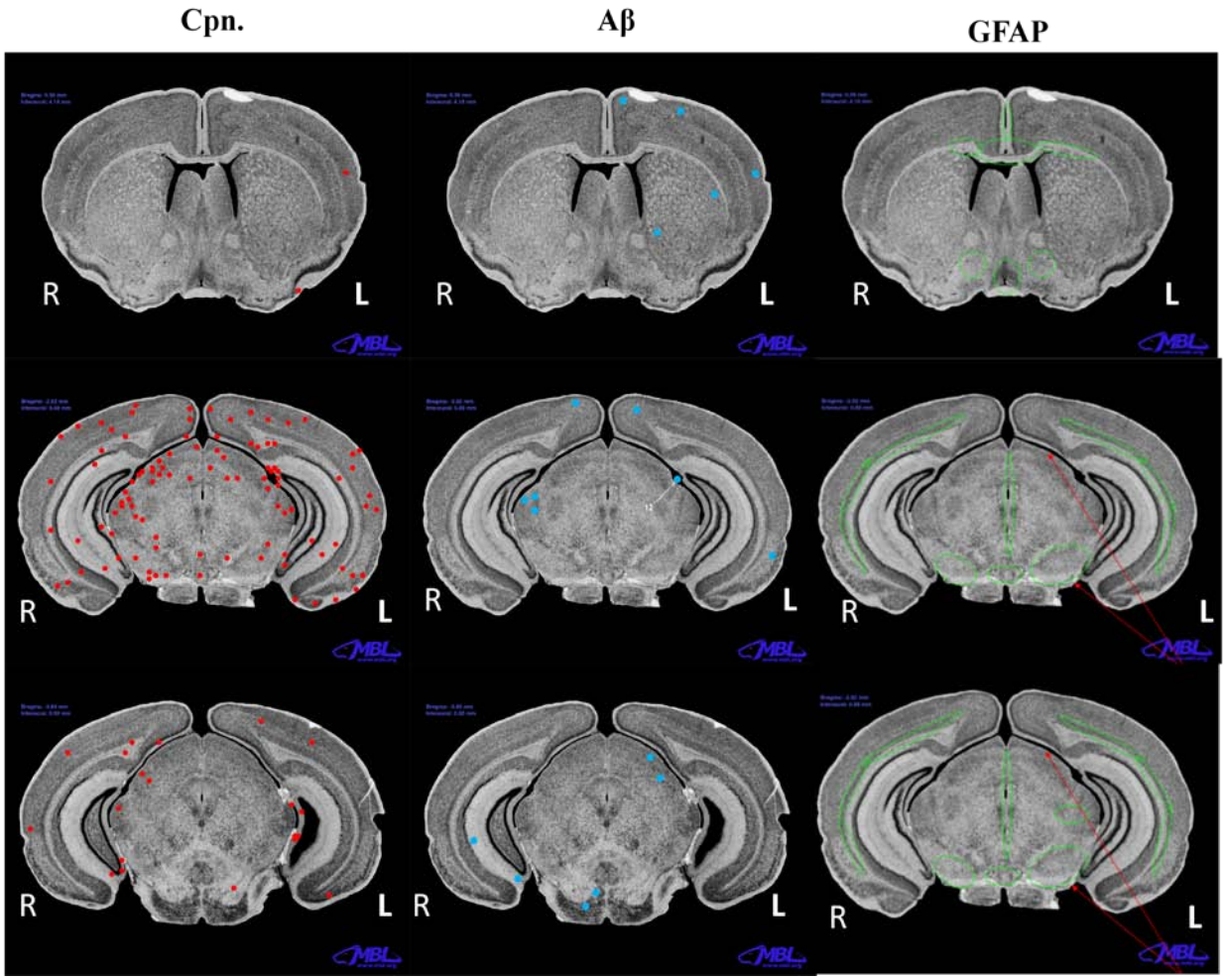

Figure 7: Distribution of *C. pneumoniae*-specific immunoreactive sites, amyloid deposits and activated glial cells at 14 days post-infection

C. pneumoniae immunoreactive sites (red dots), Aβ deposits (blue dots) and regions of the brain with glial cell labeling (green circles or red arrows) from individual slides in the day 14 group are presented here in areas of the frontal cortex, hippocampus and dentate gyrus, as well as regions not affected early on in Alzheimer's disease.

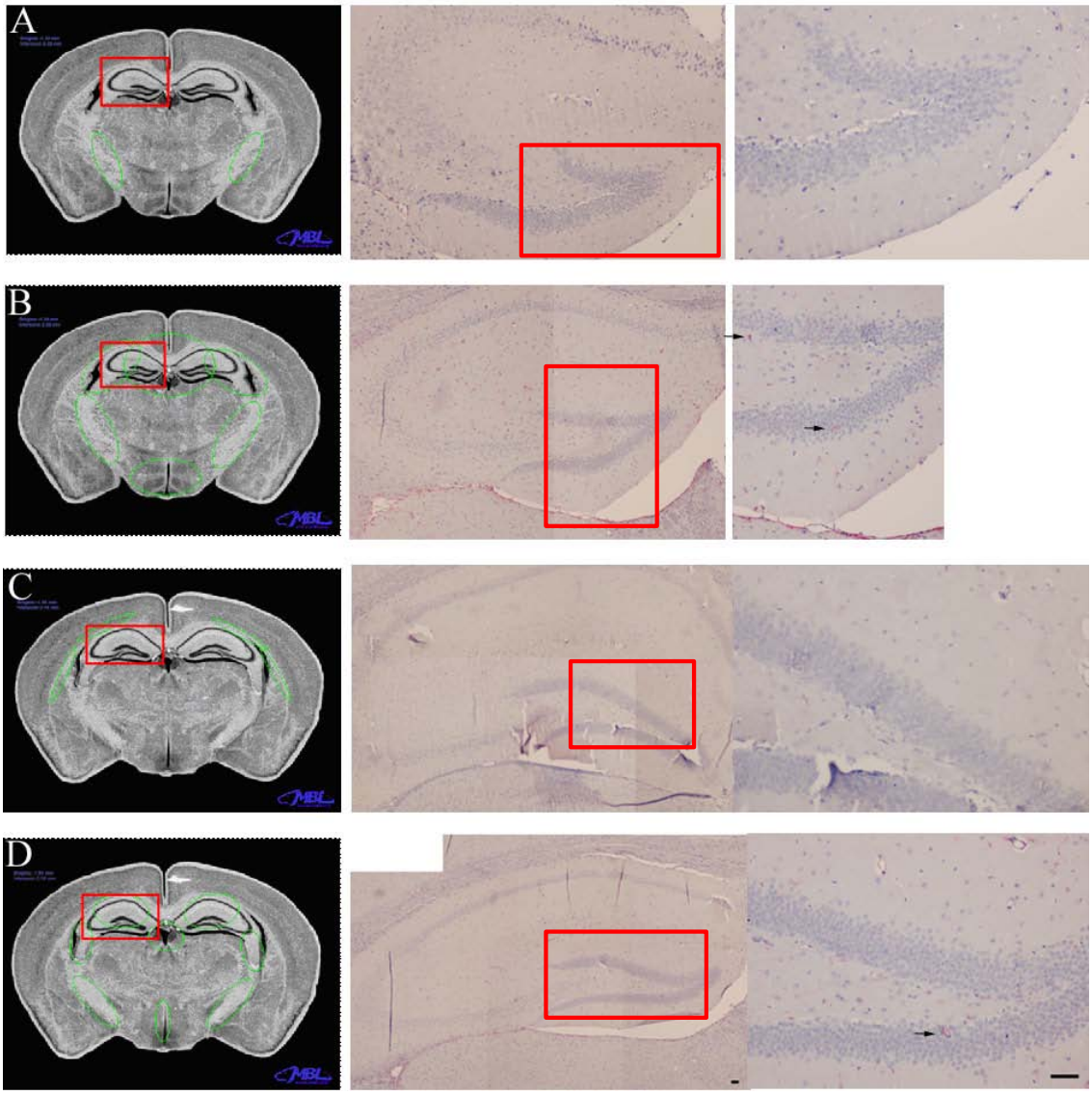

Figure 8. GFAP-specific immunoreactivity in brain tissue of infected and control mice

Regions of the brain – hippocampus and dentate gyrus, which are relevant structures in the AD brain – were selected to illustrate the difference in amount of glial cell labeling observed between a control and an experimental mouse at each time point. Substantial glial cell labeling was observed in the infected mice and comparable sections in controls were selected for comparison. The red boxes in the left column of images represent the region of the section observed at higher power, which are those located in the center column. The red boxes in the center column of images represent the region of the section observed at an additionally increased power, which are those located in the right column. A) This row represents day 7 data from an uninfected, vehicle injected control, mouse. B) This row represents day 7 data from an infected mouse. C) This row represents day 14 data from an uninfected, no-injection control, mouse. D) This row represents day 14 data from an infected mouse. (Size bar = 100 µm)

Discussion

I. Summary of Results

The brains of 8 BALB/c mice, 3 infected and 1 control for each of the two time points, days 7 and 14, were analyzed for this project (Table 1). The mice were infected, via direct intracranial injection, with a respiratory isolate (AR-39) of *Chlamydia pneumoniae*. The control mice that were analyzed were either injected with vehicle only (HBSS), day 7 group, or not injected, day 14 group. Brain tissue sections from all mice were immunolabeled and analyzed for the presence of *C. pneumoniae* antigen, amyloid plaques and activated markers in glial cells.

At 7 days post-infection the average *C. pneumoniae* antigen burden for the 3 infected mice was 68 ± 51.06. For the 3 infected mice 82% (166 of 203) of the total immunoreactive sites were identified within 0.84 mm of Bregma, the location of the injection site (Figure 3 and Table 5). For the vehicle only control mouse, 100% (27 of 27) of the *C. pneumoniae*-specific immunoreactive sites were located in this region. At day 14 post-infection, the average *C. pneumoniae* antigen burden for the 3 infected mice was 60 ± 43.79. For these mice 70% (126 of 179) of the total *C. pneumoniae*-specific immunoreactive sites were detected within 0.84 mm of Bregma (Table 5). The control mouse at this time point had 94% (17 of 18) of the *C. pneumoniae*-specific immunoreactive sites in this region.

Amyloid deposits were detected in 3 of 3 infected mice, using polyclonal Aβ-specific antibodies and detected in 2 of 3 infected mice, using the monoclonal Aβ6E10 antibody, at 7 days post-infection (Table 4). No deposits were observed in the uninfected mouse with either antibody. The average number of deposits for the infected mice at 7 days post-infection, using the Aβ 1-42 antibody, was 4 ± 2.89 and with the Aβ6E10 antibody the average number of deposits was 5 ± 4.12. For all amyloid specific immunoreactivity, 26 of 27 (96%) total amyloid deposits were detected within 0.84 mm of Bregma in the infected mice (Table 5). At 14 days post-infection, amyloid deposits were detected via immunohistochemistry in 2 of 3 infected mice, using the polyclonal Aβ-specific antibodies, and detected in 3 of 3 infected mice, using the monoclonal Aβ6E10 antibody (Table 4). Two deposits were observed in the uninfected mouse labeled with the Aβ 1-42 antibody. At 14 days post-infection, the average number of deposits for the infected mice at this time point, using the Aβ 1-42 antibody, was 5 ± 3.69 and with the Aβ6E10 antibody the average total number of deposits was 6 ± 4.32. For all amyloid specific immunoreactivity, 13 of 32 (41%) total amyloid deposits were detected within 0.84 mm of Bregma in the infected mice and 2 of 2 deposits were detected in this region in the control mouse (Table 5).

Global activation of glia was observed in the CNS of infected mice at both 7 and 14 days post-infection. The number of regions with activated glial cells was greater in the infected mice compared to uninfected controls at both time points (Figure 6). The hippocampus and dentate gyrus of an infected mouse was compared to that of a control mouse. At each time point a substantial difference in the total number of activated glial

cells was noted between the infected and uninfected mice in these regions with infected mice clearly having a greater number of activated glia (Figure 6).

II. Relationship between *C. pneumoniae*, Inflammation and Amyloid

Although the role of infection in AD is still debated, the concept of an infection playing a role in the neuroinflammatory cascade has gained increased recognition [5, 40]. Many of the laboratories that study infection and AD focus specifically on the role of infection with *C. pneumoniae* in the initiation and progression of late-onset Alzheimer's disease. The initial study in 1998 by Balin and co-workers compared human non-AD control brain tissue to AD brain tissue post-mortem [26]. In this study using RT-PCR specific for *C. pneumoniae,* they detected *C. pneumoniae* in 17 of 19 AD brains, while only 1 of 19 control brains had detectable levels of *C. pneumoniae*. In addition, *C. pneumoniae* was found in areas of typical AD neuropathology and the organism was confirmed in perivascular macrophages, pericytes and microglia. In 2000, two additional laboratories published their findings on the presence of *C. pneumoniae* in AD brain tissue [41, 42]. Mahony and co-workers found that 18 of 21 AD brains were positive for *C. pneumoniae.* Ossewaarde and co-workers found that 92% of the AD brains they analyzed were positive for *C. pneumoniae* [41, 42].

Recent studies in this laboratory [7] support previous research that indicates that *C. pneumoniae* is capable of entering the CNS following intranasal inoculation. Once *C. pneumoniae* has entered the CNS *C. pneumoniae* stimulates the deposition of amyloid [7].

To expand our understanding of the role of infection and inflammation in amyloid deposition in AD, we compared our data with data obtained from previous work in this laboratory [7]. Following intranasal inoculation with *C. pneumoniae*, the *C. pneumoniae* burden peaks at 1 month post-infection and a subsequent peak in amyloid burden occurs at 2 months post-infection. The *C. pneumoniae* burden decreased at 2, 3 and 4 months post-infection and the number of amyloid deposits decreased after 2 months and at the 3 and 4 month time points. This suggests that *C. pneumoniae* infection induces an inflammatory response and an up-regulation of Aβ production and subsequent deposition. Once the *C. pneumoniae* antigen or the infection burden decreases, the activated glia appear to reverse the process of amyloid deposition and the number of deposits decreases.

In this project at days 7 and 14 following direct intracranial injection with *C. pneumoniae*, substantial *C. pneumoniae* antigen was detected, a glial cell response was identified, and amyloid beta deposition was initiated in the infected mice. The greatest *C. pneumoniae* antigen burden was localized to regions near the injection site at day 7, but at day 14 *C. pneumoniae* was identified in more distal regions of the CNS (Table 5). At both days 7 and 14, *C. pneumoniae* was detected in both hemispheres. These data suggest that *C. pneumoniae* infection spreads from the site of injection and disseminates to more distant regions of the CNS. Following the intranasal inoculations, the *C. pneumoniae* antigen appears to be detected in the olfactory bulbs and frontal cortical regions at early time points and spreads from these areas, which are proximal to the site of inoculation, and then to other regions of the CNS more distant to the initial site of infection. Based on the route of inoculation the majority of antigen is proximal to the site of injection, and at later time points, it spreads from this location (unpublished

observations). The results obtained in this project confirm that an inflammatory response is induced in the CNS following direct intracranial infection with the organism and that infection within the CNS with the organism induces amyloid deposition.

Global glial cell activation was observed in the CNS of infected mice following direct intracranial infection. Glial cell activation was observed in regions where no *C. pneumoniae* antigen was detected. This may be in response to soluble *C. pneumoniae* antigen or possibly soluble Aβ antigen. Another group found that increased Aβ activates microglia and astrocytes and promotes the release of inflammatory mediators and amyloid deposition [9]. Previous research supports the role of soluble Aβ promoting glial cell activation and unpublished observations in this laboratory indicate that following infection with *C. pneumoniae*, high antigen burden precedes high Aβ deposits; following reduction and clearance of *C. pneumoniae* antigen, the number of Aβ deposits decreases. This suggests that in this experimental system, *C. pneumoniae* infection is the primary factor that induces and promotes amyloid deposition [7]. Glial cell activation appears to contribute to limiting *C. pneumoniae* replication and ultimately to resolving the infection in the CNS [35].

Previous findings in this laboratory indicate that *C. pneumoniae* antigen peaks 28 days post-intracranial infection and then decreases at subsequent time points (unpublished observations). At 56 days post-infection, amyloid deposition peaks and then drops at subsequent time points (days 84 and 106 days post infection), but no analysis of glial cell activation was performed in the previous studies. Others who have studied the relationship between *C. pneumoniae*, Aβ and glia have found that this organism enhances microglial activation [38]. Glia have been shown to be

chemotactically attracted to Aβ [43]. Previous research illustrates that Aβ is constitutively produced by normal neuronal cells and microglia and astrocytes appear to be involved with normal clearance [44]. *C. pneumoniae* infection serves as a stimulus for inflammation, and glial cell activation plays a role in amyloid deposit (plaque) biogenesis.

Both *C. pneumoniae* antigen and glial cell activation contribute to amyloid deposition in BALB/c mice infected via direct intracranial injection. At day 7, amyloid deposits were localized to regions near the injection site, but at day 14, the deposits were located in regions more distal to the injection site (Table 5). This parallels our observations for *C. pneumoniae* antigen at 7 and 14 days post-infection. Although amyloid deposits were identified in the infected mice, the total number was not as substantial as that found in previous studies at the time of peak deposition. At day 7 and 14 we observed approximately 4 total amyloid deposits per mouse, whereas in preceding studies (unpublished observations), the total number of deposits at the time of peak deposition (56 days post-infection) was approximately 36 per mouse. The amount of deposits we observed in this study (approximately 4 per mouse) was comparable to the day 84 time point from the previous study (approximately 6 per mouse). Although few amyloid deposits were detected, we observed global glial cell activation, likely a result of a high burden of soluble amyloid. A high burden of organism at 28 and 56 days results in accumulation of amyloid deposits [7]. Once *C. pneumoniae* antigen began to decrease, the number of amyloid deposits decreased substantially.

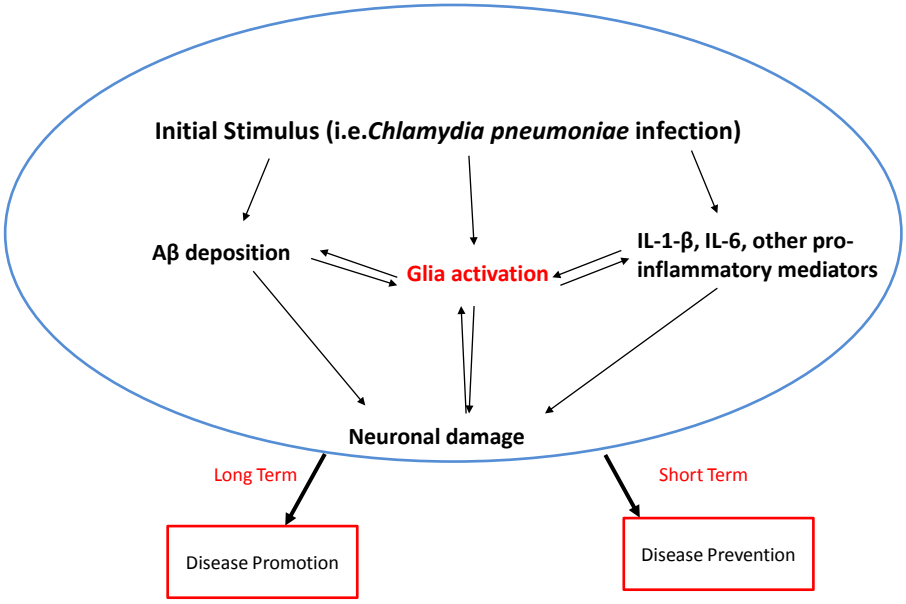

Figure 9. Contributing factors in late-onset Alzheimer's disease.

Chronic inflammation and amyloid deposition are two hallmarks of Alzheimer's disease. We hypothesized that we would observe *C. pneumoniae* antigen and glial cell activation in the CNS following direct intracranial infection with *C. pneumoniae*. We did obtain these results, but we found that *C. pneumoniae* antigen is not always present in the same regions in which we observe glial cell activation (Figure 9). Furthermore, we found substantial amounts of activated glial cells in infected mice compared to uninfected mice (Figure 6). These data suggests that the presence of *C. pneumoniae* antigen may not be the only trigger for glial cell activation in this system and that glia may be responding to the presence of soluble amyloid as well as soluble *C. pneumoniae* antigen such as lipopolysaccharide (LPS). Given that amyloid deposition was observed, we assume that

the total amyloid burden, soluble plus deposited amyloid, is high since this is consistent with previous findings. We hypothesized that amyloid deposits would be observed in regions where inflammation occurs; however, glial cell activation was not co-localized with or concentrated solely around Aβ deposits solely. This attraction was more of a global phenomenon suggesting some soluble stimulus such as *C. pneumoniae* antigen or Aβ were possible triggers for glial cell activation and inflammation, which would contribute to the formation and deposition of β amyloid.

III. Application of AD Mouse Model to AD in the Human Brain

This project supports the role of *C. pneumoniae* infection as one of the possible factors contributing to neuropathology in late-onset Alzheimer's disease. The prevalence of infection with *C. pneumoniae* in the population is about 40% and this organism can infect the same host multiple times throughout their lifetime [32, 33]. These data obtained in this study confirm those of previous studies that have shown that *C. pneumoniae* is capable of establishing an infection and producing AD-like pathology in BALB/c mice [7]. This laboratory has also studied the effects of exposing mice to *C. pneumoniae* at multiple times (unpublished observations). These data suggest that AD-like pathology increased in a step-wise fashion following multiple exposures. Thus, re-exposure may have an additive or progressive effect.

This project also confirms the ability of this organism to induce an inflammatory response in the CNS that appears to contribute to the deposition of amyloid in the brain. In addition to the presence of AD-like pathology, several inflammatory mediators have

been observed around amyloid deposits. This suggests that the inflammatory response may be contributing to the presence and onset of pathology (unpublished observations).

As all individuals age, it is important to recognize that their immune systems change and they are not as capable of fighting and clearing infections and amyloid deposits as would be younger individuals. Many studies have suggested that as we age, we are more susceptible to infections and re-exposure to an organism such as *C. pneumoniae* is a likely probability in our aging populations [45]. Individuals who are exposed to this organism may become infected, and once infected they may develop chronic inflammation in the CNS. Infection and chronic inflammation together could contribute to cumulative amounts of amyloid deposits that, over time, cannot be cleared from the CNS thus contributing to AD pathology and eventual symptomatology. Therefore, infection with an organism such as *C. pneumoniae* may be one factor that initiates an inflammatory response that could result in the neuropathology consistent with late-onset Alzheimer's disease.

IV. Future Directions

This study confirms results obtained from preceding studies in this laboratory and expands our understanding of the ability of *C. pneumoniae* to establish an infection in the CNS. Further, this infection appears to elicit an inflammatory response and contribute to the production of amyloid deposits. However, further research is necessary to determine the length of time needed, following infection with *C. pneumoniae,* to induce the processes involved in the production of AD-like pathology that may ultimately contribute

to AD symptomatology. This project illustrates the ability of *C. pneumoniae* to establish a CNS infection as early as 7 and 14 days following direct intracranial infection with the organism in the brain of a BALB/c mouse. In addition, we observed an inflammatory response as depicted by the presence of activated glial cells as well as the deposition of Aβ at both time points in the CNS of a BALB/c mouse.

Previous studies in this laboratory have found that following intranasal inoculation with *C. pneumoniae*, the highest burden of *C. pneumoniae* antigen was observed 1 month after infection and then the burden decreases at 2, 3 and 4 months post-infection [7]. In the same experiment they found that amyloid deposition was low at 1 month post-infection, but increases and peaks at 2 months post-infection, subsequently decreasing at 3 and 4 months. It seems that the greatest amount of amyloid deposition occurs after the greatest burden of *C. pneumoniae* in the CNS, which is supported by the observations in this project that found that 14 days post-infection may be too early to detect a substantial number of amyloid deposits.

In this project we saw limited deposits in the brains of BALB/c mice; however we did see an inflammatory response in the infected mice even with this minimal deposition, which indicates that other triggers for inflammation may be present in this system for studying late-onset Alzheimer's disease. Future considerations for this project should include performing an ELISA to detect the amount of soluble amyloid at each of the specified time points. Detecting the total amyloid burden, soluble plus insoluble amyloid, may contribute to our understanding of the role of soluble amyloid in glial activation and eventual deposition. Previous data indicates that in order for amyloid to deposit there must be a high total burden of amyloid. Since we saw deposits in the mice

analyzed for this project, we have hypothesized that there is a high burden of total amyloid in the CNS of the mice contributing to amyloid deposition.

One of the major limitations of this project was that there were a small number of mice analyzed for data collection. It is necessary to increase the number of mice analyzed for each time point so that statistical significance with greater power can be obtained. Also, it would be ideal to have the same number of control and experimental mice analyzed for each of the time points. For example, in this project only one control was analyzed at each time point and of those two controls one was a no injection control and the other was a vehicle only control. Analyzing more coronal sections that represent the area of the brain of interest would also be beneficial to obtain a better statistical sampling (Table 5).

As further work is completed for this project, another consideration should include increasing the number of mice analyzed at later time points following direct intracranial infection with *C. pneumoniae.* Days 28, 42 and 56 post-infection should be evaluated to determine if more amyloid deposits would be detected at greater lengths of time after infection. These time points are significant because we have collected data in previous studies at these times following intranasal inoculation [7]. In these previous projects, the analysis showed that amyloid deposition peaked following a peak in *C. pneumoniae* burden. Therefore, we may only have seen limited amyloid deposition because a limited number of sections were analyzed for these time points following infection that would determine substantial deposition.

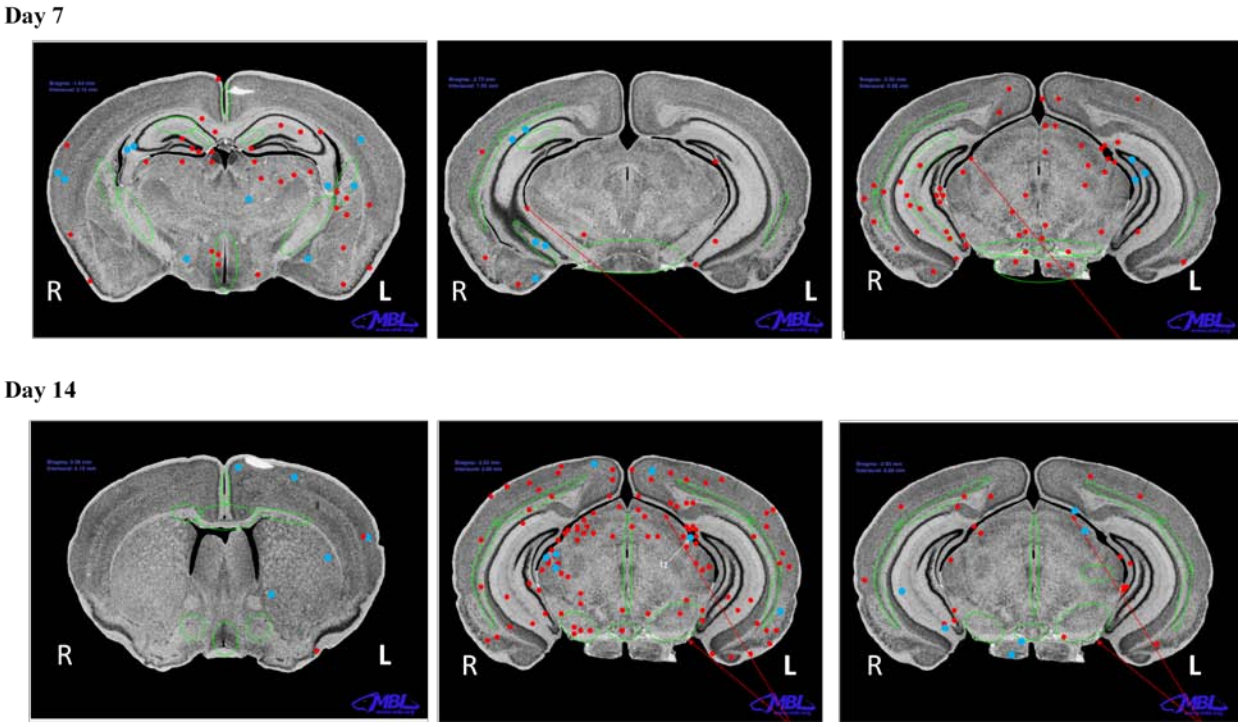

Figure 10. Relationship between *C. pneumoniae-specific* immunoreactive sites, amyloid deposits and activated glial cells

The red dots represent C. pneumoniae antigen, the blue dots represent amyloid beta deposition (labeled with either Aβ 1-42 or Aβ6E10 antibody – Materials and Methods subsection *Antibodies*) and the green circles and red arrows represent glia labeling.

References

1. Baron R, Harpaz I, Nemirovsky A, Cohen H, Monsonego A: **Immunity and neuronal repair in the progression of Alzheimer's disease: a brief overview.** Exp Gerontol 2007, **42**(1-2):64-69.

2. Blennow K, de Leon MJ, Zetterberg H: **Alzheimer's disease.** Lancet 2006, **368**(9533):387-403.

3. Kumar V, Abbas A, Fausto N: *Robbins and Cotran Pathologic Basis of Disease:* 8th ed. Philadelphia, PA: Elsevier Saunders; 2007.

4. Anonymous *Sherris Medical Microbiology: An Introduction to Infectious Diseases:* 4th ed. McGraw Hill Companies, Inc.; 2004.

5. Balin BJ, Appelt DM: **Role of infection in Alzheimer's disease.** J Am Osteopath Assoc 2001, **101**(12 Suppl Pt 1):S1-6.

6. Hoozemans JJ, Veerhuis R, Rozemuller JM, Eikelenboom P: **Neuroinflammation and regeneration in the early stages of Alzheimer's disease pathology.** Int J Dev Neurosci 2006, **24**(2-3):157-165.

7. Little CS, Hammond CJ, MacIntyre A, Balin BJ, Appelt DM: **Chlamydia pneumoniae induces Alzheimer-like amyloid plaques in brains of BALB/c mice.** Neurobiol Aging 2004, **25**(4):419-429.

8. Ropper AH, Samuels MA: *Adams & Victor's Principles of Neurology:* 9th ed. McGraw Hill Companies, Inc.; 2009.

9. Schlachetzki JC, Hull M: **Microglial activation in Alzheimer's disease.** Curr Alzheimer Res 2009, **6**(6):554-563.

10. Naslund J, Schierhorn A, Hellman U, Lannfelt L, Roses AD, Tjernberg LO, Silberring J, Gandy SE, Winblad B, Greengard P: **Relative abundance of Alzheimer A beta amyloid peptide variants in Alzheimer disease and normal aging.** Proc Natl Acad Sci U S A 1994, **91**(18):8378-8382.

11. Boelen E, Stassen FR, van der Ven AJ, Lemmens MA, Steinbusch HP, Bruggeman CA, Schmitz C, Steinbusch HW: **Detection of amyloid beta aggregates in the brain of BALB/c mice after Chlamydia pneumoniae infection.** Acta Neuropathol 2007, **114**(3):255-261.

12. Roses AD: **Apolipoprotein E alleles as risk factors in Alzheimer's disease.** Annu Rev Med 1996, **47**:387-400.

13. Balin BJ, Little CS, Hammond CJ, Appelt DM, Whittum-Hudson JA, Gerard HC, Hudson AP: **Chlamydophila pneumoniae and the etiology of late-onset Alzheimer's disease.** J Alzheimers Dis 2008, **13**(4):371-380.

14. Lomen-Hoerth C, Messing RO: **Chapter 7: Nervous System Disorders.** In *Pathophysiology of Disease: An Introduction to Clinical Medicine.* 6th edition. Edited by Anonymous The McGraw Hill Companies; 2010:.

15. Farrer LA, Cupples LA, Haines JL, Hyman B, Kukull WA, Mayeux R, Myers RH, Pericak-Vance MA, Risch N, van Duijn CM: **Effects of age, sex, and ethnicity on the association between apolipoprotein E genotype and Alzheimer disease. A meta-analysis. APOE and Alzheimer Disease Meta Analysis Consortium.** JAMA 1997, **278**(16):1349-1356.

16. Jicha GA, Carr SA: **Conceptual evolution in Alzheimer's disease: implications for understanding the clinical phenotype of progressive neurodegenerative disease.** J Alzheimers Dis 2010, **19**(1):253-272.

17. Cummings JL, Benson DF: *Dementia: A Clinical Approach:* 2nd ed. Stoneham, MD: Butterworth-Heinemann, Reed Publishing (USA) Inc.; 1992.

18. Braak H, Braak E: **Neuropathological stageing of Alzheimer-related changes.** Acta Neuropathol 1991, **82**(4):239-259.

19. Nolte J: *The Human Brain: An Introduction to Its Functional Anatomy:* 5th ed. St. Louis, MO: Mosby Inc.; 2002.

20. Braak E, Griffing K, Arai K, Bohl J, Bratzke H, Braak H: **Neuropathology of Alzheimer's disease: what is new since A. Alzheimer?** Eur Arch Psychiatry Clin Neurosci 1999, **249 Suppl 3**:14-22.

21. Hardy JA, Higgins GA: **Alzheimer's disease: the amyloid cascade hypothesis.** Science 1992, **256**(5054):184-185.

22. Maccioni RB, Munoz JP, Barbeito L: **The molecular bases of Alzheimer's disease and other neurodegenerative disorders.** Arch Med Res 2001, **32**(5):367-381.

23. Appelt DM, Roupas MR, Way DS, Bell MG, Albert EV, Hammond CJ, Balin BJ: **Inhibition of apoptosis in neuronal cells infected with Chlamydophila (Chlamydia) pneumoniae.** BMC Neurosci 2008, **9**:13.

24. Akiyama H, Barger S, Barnum S, Bradt B, Bauer J, Cole GM, Cooper NR, Eikelenboom P, Emmerling M, Fiebich BL, Finch CE, Frautschy S, Griffin WS, Hampel H, Hull M, Landreth G, Lue L, Mrak R, Mackenzie IR, McGeer PL, O'Banion MK, Pachter J, Pasinetti G, Plata-Salaman C, Rogers J, Rydel R, Shen Y, Streit W, Strohmeyer R, Tooyoma I, Van Muiswinkel FL, Veerhuis R, Walker D, Webster S, Wegrzyniak B, Wenk G, Wyss-Coray T: **Inflammation and Alzheimer's disease.** Neurobiol Aging 2000, **21**(3):383-421.

25. Santana S, Recuero M, Bullido MJ, Valdivieso F, Aldudo J: **Herpes simplex virus type I induces the accumulation of intracellular beta-amyloid in autophagic compartments and the inhibition of the non-amyloidogenic pathway in human neuroblastoma cells.** Neurobiol Aging 2011, .

26. Balin BJ, Gerard HC, Arking EJ, Appelt DM, Branigan PJ, Abrams JT, Whittum-Hudson JA, Hudson AP: **Identification and localization of Chlamydia pneumoniae in the Alzheimer's brain.** Med Microbiol Immunol 1998, **187**(1):23-42.

27. Gerard HC, Dreses-Werringloer U, Wildt KS, Deka S, Oszust C, Balin BJ, Frey WH,2nd, Bordayo EZ, Whittum-Hudson JA, Hudson AP: **Chlamydophila (Chlamydia) pneumoniae in the Alzheimer's brain.** FEMS Immunol Med Microbiol 2006, **48**(3):355-366.

28. Forbes BA, Sahm DF, Weissfeld AS: *Bailey & Scott's Diagnostic Microbiology:* 11th ed. St. Louis, MO: Mosby Inc.; 2002.

29. Hatch TP: *Chlamydia: Intracellular Biology, Pathogenesis, and Immunity:* Washington, D.C.: ASM Press; 1999.

30. Mannonen L, Nikula T, Haveri A, Reinikainen A, Vuola JM, Lahesmaa R, Puolakkainen M: **Up-regulation of host cell genes during interferon-gamma-induced persistent Chlamydia pneumoniae infection in HL cells.** J Infect Dis 2007, **195**(2):212-219.

31. Moazed TC, Kuo CC, Grayston JT, Campbell LA: **Evidence of systemic dissemination of Chlamydia pneumoniae via macrophages in the mouse.** J Infect Dis 1998, **177**(5):1322-1325.

32. Stamm WE: *Harrison's Priniciples of Internal Medicine: Chlamydial Infections:* 17th ed. McGraw Hill Companies, Inc.; 2008.

33. Schachter J: *Chlamydia: Intracellular Biology, Pathogenesis, and Immunity:* Washington, D.C.: ASM Press; 1999.

34. Muhlestein JB, Hammond EH, Carlquist JF, Radicke E, Thomson MJ, Karagounis LA, Woods ML, Anderson JL: **Increased incidence of Chlamydia species within the coronary arteries of patients with symptomatic atherosclerotic versus other forms of cardiovascular disease.** J Am Coll Cardiol 1996, **27**(7):1555-1561.

35. Glass CK, Saijo K, Winner B, Marchetto MC, Gage FH: **Mechanisms underlying inflammation in neurodegeneration.** Cell 2010, **140**(6):918-934.

36. Wirths O, Breyhan H, Marcello A, Cotel MC, Bruck W, Bayer TA: **Inflammatory changes are tightly associated with neurodegeneration in the brain and spinal cord of the APP/PS1KI mouse model of Alzheimer's disease.** Neurobiol Aging 2010, **31**(5):747-757.

37. Heneka MT, Sastre M, Dumitrescu-Ozimek L, Dewachter I, Walter J, Klockgether T, Van Leuven F: **Focal glial activation coincides with increased BACE1 activation and precedes amyloid plaque deposition in APP[V717I] transgenic mice.** J Neuroinflammation 2005, **2**:22.

38. Voorend M, van der Ven AJ, Mulder M, Lodder J, Steinbusch HW, Bruggeman CA: **Chlamydia pneumoniae infection enhances microglial activation in atherosclerotic mice.** Neurobiol Aging 2010, **31**(10):1766-1773.

39. [www.mbl.org]

40. Honjo K, van Reekum R, Verhoeff NP: **Alzheimer's disease and infection: do infectious agents contribute to progression of Alzheimer's disease?** Alzheimers Dement 2009, **5**(4):348-360.

41. Mahony J, Woulfe J, Munoz D, Browning D, Chong S, Smieja M: **Identification of Chlamydia pneumoniae in the Alzheimer's brain.** *World Alzheimer Congress* 2000, **7:**.

42. Saikku P (Ed): *Proceedings of the Fourth Meeting of the European Society for Chlamydia Research: August 20-23;* Helsinki, Finland: 2000.

43. Rogers J, Lue LF: **Microglial chemotaxis, activation, and phagocytosis of amyloid beta-peptide as linked phenomena in Alzheimer's disease.** Neurochem Int 2001, **39**(5-6):333-340.

44. Giulian D, Haverkamp LJ, Yu JH, Karshin W, Tom D, Li J, Kirkpatrick J, Kuo LM, Roher AE: **Specific domains of beta-amyloid from Alzheimer plaque elicit neuron killing in human microglia.** J Neurosci 1996, **16**(19):6021-6037.

45. Yoshikawa TT, Norman DC: *Infectious disease in the aging: a clinical handbook:* Humana Press; 2001.